

K Bharathi<sup>1</sup> and A. S. Arunachalam<sup>2</sup>

<sup>1</sup>Research scholar, Department of Computer Science, Vels Institute of Science, Technology and Advanced Studies (VISTAS), Chennai, India.

<sup>2</sup>Associate Professor, Department of Computer Science, Vels Institute of Science, Technology and Advanced Studies (VISTAS), Chennai, India.

<sup>2</sup>arunachalam.scs@vistas.ac.in

**Abstract**—Breast Cancer is considered to be the deadliest disease among women due to the carcinoma in epithelial tissue development in breast. The cause of the disease many vary due to many circumstances, but identification procedure followed are mostly similar. The clinical way of identifying the cancer effected tissues in breast are followed in advance stages or pre advanced stages, which is due to the lack of adequate knowledge about breast cancer. The treatment given during the final stages are mostly not feasible solution and eventually ends with negative result. Digital Image Processing (DIP) technique coupled with Data Mining and Machine learning algorithms are most recently used breast cancer identification procedure. The identification procedure followed using those techniques are not only accurate, it also gives very fast analyzing report based on the historical record. This research article proposes pre-processing technique, which is a part of the overall research work of breast cancer identification procedure. The Mammography images collected from the source may contains many irrelevant information as well as missing values. The article gives a clear idea of pre-processing techniques followed as well as filtering techniques implemented to enhance the quality of the collected breast cancer Mammography images.

**Keywords**—Image Enhancement; Gaussian noise Removal; Speckle noise Removal; Wiener Filter; Median Filter; Gaussian Filter;

## Introduction

The Breast carcinoma images are collected from various sources are to be cleaned before taking the images into the analyzing stage. The initial noise removal techniques are applied for removing the irrelevancy presence in the collected images. The unclear and unwanted objects present in the images re removed unconditionally to prevent the inaccurate prediction results. The pre-processing plays a major role in increasing the probability chance of accuracy as well as for improving the quality of the collected images. The raw breast cancer Mammography images are taken to the preprocessing stage, where initial cleaning process is carried out for improving the final accuracy.

The dimensions of the images are normally determined with pixel representations, which is common in all digital images. DIP gives a benefit of easy transformation, processing and storing the image into human understandable record for easy prediction. The DIP gives a clear and enhanced quality images for easy identification and prediction process. In recent years many diagnostics centers and radiologist started to deploy the DIP technology in the medical applications.

Some of the advantages of using DIP in medical image processing are listed below

- i) Easy Image enhancement / restoration
- ii) Medical image visualization
- iii) Artistic effects after processing
- iv) Industrial inspection for testing purpose
- v) Law enforcement for legal rules

Imaging technology plays a major role in medical field to diagnose patents internal organs without clinical cut or operations. This fields also helps major surgent to clearly visualize the inner and deep wounds without opening the body. The DIP helps in finding the carcinoma in epithelial tissue growth very clearly and gives clearcut idea of the severity level of infection or growth.

This research article focuses on cleaning the irrelevancy in collected Mammography breast cancer images with the usage of DIP processing techniques, which makes the breast cancer identification accurately. The processed images after the preprocessing stages are taken for applying the filtering methodology for enhancing the quality of the pre-processed images. The segmentation techniques followed after the pro-processing helps the specialist to identify the severity level of the growth in early stage of breast cancer.

The image enhancement procedure is followed after the pro-processing technique to enhance the quality of the processed images. The noise present in the images is also removed before the segmentation stage. The noise removing techniques removes all the cancer affected parts from the mammography breast cancer images. Machine learning and deep learning algorithms are used further to analyze the severity of the cancer growth in the breast.

The research article is organized as follows. Section 1 gives an introduction to the area of image processing and breast cancer affects. The significance of the research work is also discussed in this section. Section 2 gives complete literature review about the latest research work undergone in the area of breast cancer detection using digital image processing. Section 3 clearly explains the materials and methods for implementing the proposed research work. Section 4 gives a detailed explanation about the obtained results for the breast cancer pre-processing stage with clear future goals. The final part of the research article explains the conclusion part, where the future work is explained.

## REVIEW OF LITERATURE

In histopathologic image problems, it is more typical nowadays to employ some type of preprocessing. In [38], the authors give a thorough review of graph-based deep learning in computational histopathology. They mention that stain normalization is widely practiced when applying standard entity graph pathology workflows. Likewise, in [39] stain normalization is employed as preprocessing to a classification model which not only predicts histological sub-types of endometrial carcinoma but also molecular sub-types and 18 common genetic mutations from histopathological images.

Tumor segmentation in lung cancer images is discussed in [40], where the authors use staining normalization during preprocessing to normalize image appearance. A modified Gaussian filter is then applied as a form of color augmentation to improve the robustness of the utilized models. A binary classification task for breast cancer images is investigated in [41], with an accuracy rate over 98%. The suggested method adopts a three-stage pipeline: preprocessing, segmentation, and classification. In the preprocessing stage, fuzzy histogram equalization is used to retain local image details while avoiding the effects of over-enhancement and noise growth.

Segmentation of tumors in cervical cancer images is considered in [42], with the authors suggesting an automatic preprocessing architecture with the goal of enhancing image quality and consequently improving model performance. This paradigm employs a host of preprocessing methods, such as adaptive histogram equalization, Gaussian filtering, and sharpening filters. In [43], an analytical study is given on the use of various filtering methods on retinal fundus images. The filters tested are Contrast Limited Adaptive Histogram Equalization (CLAHE), Adaptive Histogram Equalization (AHE), median filtering, Gaussian filtering, Wiener filtering, and adaptive median filtering. The study outlines the strengths and limitations of each method, providing concise explanations for their application.

Each filter's efficiency is measured in terms of Mean Squared Error (MSE) and Peak Signal-to-Noise Ratio (PSNR). It is evident through the results that the adaptive median filter performs the best with the highest PSNR and lowest MSE. Several deep learning models, such as VGG16, VGG19, ResNet50, MobileNet, and DenseNet121, among others [44–46], have been extensively used for histopathological image analysis. In [47], the authors introduce a cascaded deep learning model for precise nuclei segmentation from digitized histology slide images, applying the VGG16 architecture and a soft Dice loss function. In a different study [48], feature vectors of the 6B-Net and ResNet50 models are combined to achieve multi-class classification of breast cancer images. A review in [44] further discusses some of the most popular deep learning algorithms like Convolutional Neural Networks (CNNs), Generative Adversarial Networks (GANs), and Graph Neural Networks (GNNs) with special importance given to their applications in pathology.

Various researchers have used mammogram images to detect cancer. For example, the paper described in [7] suggests a deep learning-based method for the detection of breast cancer

from mammograms. Experiments were carried out using the Mammograms MIAS dataset, which includes 322 images—189 normal and 133 abnormal. Abnormal cases normally showed asymmetry, with one breast showing a dense mass. Every image was originally of 1024×1024 pixel resolution. During model development, a 70:30 train-test split was used.

The method to be used is a two-stage process. In the training stage, images went through preprocessing procedures like noise removal using morphological operations prior to being fed into a Convolutional Neural Network (CNN) for feature extraction. In the testing stage, new images were preprocessed in a similar manner and then run through the trained CNN to make predictions. The system was developed using MATLAB 2017, with a classification accuracy of 65%.

A similar method is outlined in [41], in which the authors created an automated system for detection, analysis, and classification of microcalcifications in a dataset of 990 images gathered from two medical facilities. The work also compares the performance of manually crafted features versus those obtained using deep learning, eventually merging the two for better classification accuracy.

The general approach was split into three primary stages. First, regions of interest (ROIs) with suspicious regions were acquired using an automated image pre-processing process. In the second stage, radiomics features were manually designed, including statistical, morphological, and textural features. These were supplemented by deep features taken from a fine-tuned, pre-trained Convolutional Neural Network (CNN). Lastly, during the classification stage, a Support Vector Machine (SVM) model was trained and tested based on different sets of features: handcrafted, deep, combined, and filtered. To register mammography images and extract calcifications, ROI extraction algorithms were applied. This was done through a coarse segmentation method to locate areas of interest. Morphological erosion was utilized to remove peripheral breast pixels, after which top-hat filtering was used to increase local contrast. The resulting grayscale images were thresholded to binary, dilated, and the calcification region identified as the largest connected component.

Concurrently, a CNN architecture for deep feature extraction was created. The five-layer convolutional structure used unique filters in each of its layers, and AlexNet was the baseline model for representing features. To prevent overfitting, an off-the-shelf ImageNet model was utilized. In addition, Canonical Correlation Analysis (CCA) was utilized for the fusion of handcrafted features and deep features. Utilizing this combination of CNN-based features with morphological filtering, an accuracy of 88.59% was achieved.

A pertinent study in [42] examined the performance of different neural network models under two training strategies: pre-trained weights and randomly initialized weights. The comparative study identified differences in effectiveness between the two strategies.

A deep Convolutional Neural Network (CNN) was used to assess mass lesions in mammograms from two datasets: DDSM-400, composed of 400 mass regions of interest (ROIs) extracted, and DDSM-upgraded, comprising 10,239 images.

Mass-specific cases only were chosen, providing 1,319 ROIs to train and 378 to test. A fixed-size kernel was employed to clip each lesion, keeping the mass centrally located inside the cropped region.

Data augmentation methods, such as rotation and flipping, were used to improve model performance and robustness. During the performance test, fine-tuning with transfer learning with ResNet-50 and ResNet-101 had an accuracy of 85% on both datasets. Models trained from scratch, however, had lower performance—though AlexNet, when trained from scratch, still performed well. A similar study is outlined in [43]. The authors designed an eight-layer Convolutional Neural Network (CNN) with two enhancement mechanisms: batch normalization (BN) and dropout (DO). Instead of the common max pooling, they used rank-based stochastic pooling (RSP). This all combined to create the BDR-CNN architecture—made up of CNN, BN, DO, and RSP. For further improving performance, BDR-CNN was coupled with a two-layer Graph Convolutional Network (GCN) and created the model BDR-CNN-GCN, which was used for analysis of breast mammography.

The BDR-CNN-GCN method was tested ten times on the mini-MIAS database and had an average accuracy of  $96.10\% \pm 1.60\%$ , with a sensitivity of 96% and specificity of 96%. A similar study is explained in [44], wherein the authors classified mammograms from an augmented database using transfer learning and CNN-based approaches. AlexNet was used for feature map extraction, attaining an area under the receiver operating characteristic curve (AUC) of 0.73 with data augmentation and 0.62 without data augmentation.

## MATERIALS AND METHODS

Some methods are implemented in the chosen picture data set within the image processing application domains for image preprocessing. The overall aim of this process is to develop a means for enhancing lung images that may be utilized for further diagnosis. The chosen digital MRI has proved to be the most effective technique for early detection of lung cancer. The MRI images taken in real-time for this study were provided by Gemini Scans [9]. The images are categorized into MRI pairs, each of which is a patient's left and right lungs. The data set includes photos that belong to two categories: malignant and beige.

An image enhancement technique is a method of processing an image so that the final product is far more appropriate for a given application than the original image. With the aid of the MATLAB software, the stored digital image is improved [10]. Figure 1 shows the suggested strategy.

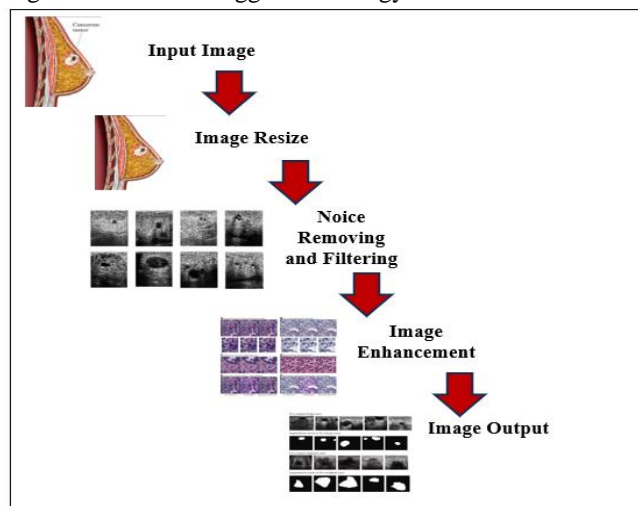


Figure 1. Preprocessing Methodology

The preprocessing method recommends the following processes: concurrent, noise elimination, filtering, and enhancement of contrast.

1. The real-time MRI image is supplied by the Gemini scan center.
2. The colour image is converted to a greyscale image.
3. Various sizes are enhanced on the photos.
4. Several methods of filtering are utilized to remove noise from the grey image.
5. The Adaptive Histogram Equalization filtering method enhances the contrast of the image.
6. The enhanced output image is the one that was obtained.

## PRE-PROCESSING

Due to various noises present in them, the raw images collected from the scan center and websites are not fit to be processed directly. Therefore, it is pre-processed prior to examination. Labelling, artefact removal, enhancement, and segmentation form a crucial step in MRI [11]. Preprocessing involves image resizing, conversion, reduction of noise, and improvement of quality, which results in an image that enables the precise identification of minute details [20].

**Gray Scale Conversion:** Filtering techniques such as power spectra and blur filters are adjusted for eliminating noise. It is obvious that the Wiener filter is divided into two different components: the inverse filtering component and the noise smoothing component. Besides employing inverse filtering (high pass filtering) for de-convolution, it even employs a

compression operation (low pass filtering) to remove noise [28].

**Image resizes:** For enlarging and shrinking the given image size in pixel form, image scaling is a significant role to play in image processing methods. Image down-sampling and image up-sampling are the two forms of image interpolation needed while resizing the data to the size of the output display or to a specific communication channel [12].

Presenting the final visual information might involve an approximate representation of the original high-resolution, even when it is more efficient to send low-resolution versions to the client. In most applications, ranging from consumer products to critical positions in the security, defence, and medical sectors, a correct scaling of image information is a required initial step. In this section, the nearest neighbour algorithmic method was employed as part of the image scaling method [25]. The nearest neighbour method's use accelerates the image processing process towards the end. The method which may be used to assess the speed of resizing is marred by the fact that the final image often has block artefacts, which are hardly perceptible to the human eye but also cause significant deterioration in error calculations applied to compare approaches. Bi-linear and bi-cubic interpolation are two other commonly used methods [13].

**Noise Removal:** Random variation of color data or intensity in images formed by scanners or medical devices is referred to as image noise. By and large, image noise is regarded as an unwanted secondary product of image formation. A measure of the doubt or lack of sureness about a signal resulting from random changes in the signal is loosely referred to as noise [14]. The variability has diverse etiology. Visual noise is to be found in all medical imaging. A noisy image looks mottled, grainy, textured, or snowy. There are several types of noise, and the most common one in medical imaging is detailed below.

**Salt and pepper:** As part of image noise removal methods, salt and pepper image conversion is widely used [24]. It occurs in the form of black and white pixels which appear randomly. When there are short transients, such as improper switching, salt and pepper noise seeps into images. It is sometimes called "spike noise" or "impulsive noise."

**Gaussian:** The Gaussian distribution, also known as statistical noise, is statistical noise with a normal distribution probability density function (PDF) [15]. Each pixel in the image will be changed from its original value by a (usually) small amount when there is Gaussian noise.

**Shot or Poisson:** The most common noise in the brighter regions of an image is referred to as short noise, or Poisson noise. Photon shot noise is another name for the statistical quantum fluctuations that an image sensor normally generates, which vary the number of photons detected at a given exposure [23].

**Speckle:** The image quality of active radar and synthetic aperture radar is degraded by speckle noise, a grainy disturbance present in both [16]. Ultrasonic medical devices are generally the source of this type of noise.

## FILTERING METHODS

To enhance an image, filters are used primarily to either repress the high frequencies of the image, which smooths the image, or its low frequencies, which enhances or detects the edges of the image [17]. An image can be filtered, for example, to emphasize specific characteristics or remove others. There are numerous ways to do this, and the most effective may depend on the image and the purpose for which it is being used. There are several applications for image filtering, including edge detection, noise filtering, sharpening, and smoothing.

**Wiener:** Inverse filtering and noise smoothing are best traded off by wiener filtering. It reverses the blurring and removes the extra noise simultaneously. When the mean square error is considered, the Wiener filtering is the best. In other words, it minimizes the overall mean square error in the process of noise smoothing and inverse filtering [18]. The Wiener filter linearly estimates the original image. A stochastic model forms the basis for the technique. The Wiener filter in the Fourier domain can be written as below, based on the orthogonality principle:

$$f(x, y) = \frac{H * (f_1, f_2) S_{xx}(f_1, f_2)}{H(f_1, f_2) 2S_{xx}(f_1, f_2) + S_{nn}(f_1, f_2)}$$

**Median:** It impacts a rectangular area through the use of the median filter. When filtering images, it adjusts photo sizes by certain conditions stated below. The median position within the 3-by-3 neighbourhood about each pixel from the input pictures is held by every output pixel. zeros play the image edges' place instead [19]. The value of the current pixel at (x,y), the point on which S is currently centered, is substituted with a single value that is the output of the filter. The notation employed is as follows.

$$Z_{min} = \text{Minimum pixel value in } S_{xy}$$

$$Z_{max} = \text{Maximum pixel value in } S_{xy}$$

$Z_{med}$  = Median pixel value in  $S_{xy}$

$Z_{xy}$  = Pixel value at co – ordinates (x,y)

$S_{max}$  = Maximum allowed size of  $S_{xy}$

Edges are not blurred and images are preserved when non-repellent noise is removed from two-dimensional signals by smoothing it out with median filtering. This renders it extremely suitable for enhancing MRI images. To determine which pixels in an image have been affected by impulsive noise, the median filter applies spatial processing. By contrasting each pixel within the image to its surrounding pixels, the median filter identifies which pixels are noise. Both the neighborhood size and comparison threshold are alterable. Impulse pixels are those that are dissimilar to most of their neighbors and are not physically coincident with those comparable to them [19]. The median pixel value of the nearby pixels that passed the noise labelling test is then used to replace these noise pixels.

**Gaussian:** The most important element of both theory and applications is the Gaussian filter. One common image filtering approach is Gaussian filtering, which is a WAP with weight defined as

$$W_{ij} \alpha \exp(-\|x_i - x_j\|), i \neq j$$

$W_{ij} = 0$ , in which  $L_2$  controls the range of the steep decline. In fact, Gaussian smoothing is a local filtering method. Gaussian filter is a prominent image denoising technique which oversmoothed images at the expense of most detail loss, especially the sharpness of edges [21]. Gaussian smoothing, or low-pass filtering, retains the low-frequency aspects of the image, which do not significantly change, but eliminates high-frequency features, including noise and edges [20]. In other words, everything that is smaller than the feature of the image gets blurred by the filter.

**Contrast Enhancement:** The contrast is the difference between the maximum and minimum pixel intensities. The formula for expanding the image histogram to increase contrast is

$$g(x, y) = \frac{f(x, y) - f_{min}}{f_{max} - f_{min}} * 2^{bpp}$$

The equation requires greyscale levels multiplied by the lowest and highest pixel intensity. As our example picture is 8 bpp, the grey levels would be 256.

The minimum value is 0 and the maximum value is 225. So the 0 is the minimum and 225 is the maximum. In this case, the formula is

$$g(x, y) = \frac{f(x, y) - 0}{225 - 0} * 255$$

$f(x,y)$ , where  $f$  is the intensity value of every pixel. In a picture, we will calculate this formula for every  $f(x,y)$ .

The capability of the image is enhanced as the equations are used. The main objectives of the contrast enhancement system are two-fold: equalisation and removal of unwanted objects, such as noise and blocking objects, with a locally adaptive histogram [22]. Specifically, block-based processing involves local adaptation, overlapping adjacent blocks minimises blocking artefact, and spatiotemporally adaptive filtering eliminates noise. Without considering the image boundary, the block-overlapped histogram equalisation algorithm's details are summarised as follows.

Figure 3 explains the correspondence between the full image and the (m,n) block. The corresponding  $B \times B$  block is subjected to histogram equalisation, and the centre pixel intensity of the block is adjusted according to the equalisation. We just add the last column of the new block and remove the first column of the old block to compute the histogram of the next block, or (m, n+1) block [26].

## EXPERIMENTAL RESULTS AND DISCUSSION

**Image resizing:** Alter the image size (in pixels). In both the horizontal and vertical directions, picture down sampling, or resampling at a lower rate, reduces a 512x512 image to 256x256, which is a factor of 2. An enlarged image is produced from a smaller one by image upsampling, or resampling at a higher rate (512x512 -> 1024x1024).

Shrink the image size and turn everything into 1D. A two-dimensional image can be reduced in two steps: first along the x direction and then along the y direction. Pixels are reduced by a factor of  $a < 1$ ; fat pixels are size  $1/a$ ; the (rescaled) target image size is  $aw$  ( $1/a = w =$  the original size (though pixel size differs)).

A "tiny pixel" has size  $1/a$ , and a rescaled target image has size  $aw$  ( $1/a = w =$  original size). Image stretching is achieved by the factor of  $a > 1$ .

Figure 2(a1,2,3,4) has the original Mammography breast cancer images for the preprocessing that was carried out for this research work. Preprocessing techniques are employed, such as image scaling, noise reduction, filtering, and contrast

enhancement. Figures 2(b1) to 2(b4) shows the representation of the images resized into 128x128 size. Figure 2(c1) to 2(c4) represented in the table shows the images resized into 256 x 256. Finally, the resizing of 512 x 512 size is represented in figure 2(d1) to 2(d4).

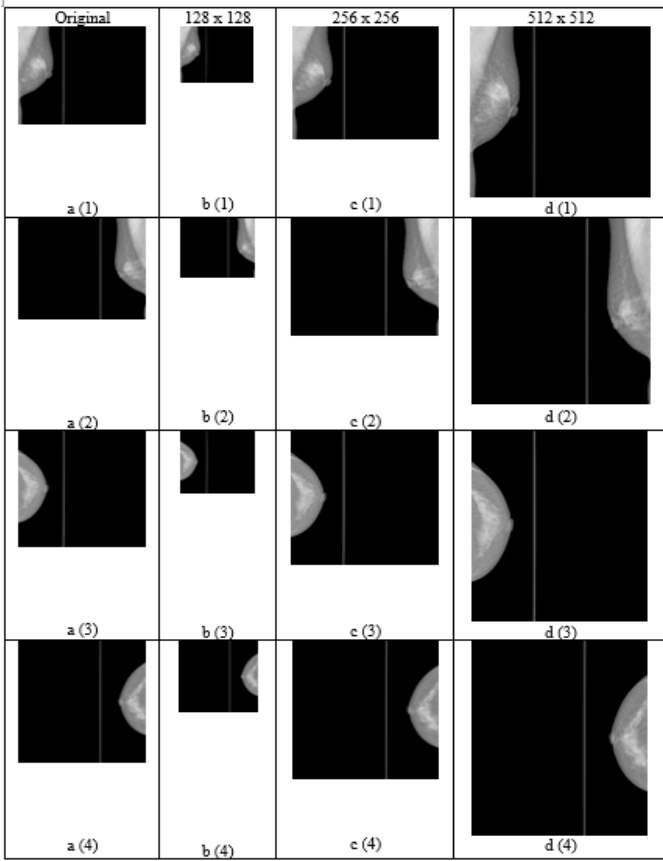


Figure 2. Results of Image Sizes

The images present in the figure 2 are taken from two different patents, which is shown from the different dimensions. The pixel range of the original images are huge in numbers, which can make the proposed model to take more running time. The preprocessing technique followed in this research article can give a proper solution in reducing the size of the image without changing the clarity of the images.

Image Size	Image Name	Space Occupied (KB)	No. of Pixels
227X222	a (1)	118.24	118,336
	a (2)	107.49	125,296
	a (3)	76.11	76,176
	a (4)	68.78	68,644
128x128	b (1)	2.55	324
	b (2)	2.33	289
	b (3)	1.93	256
	b (4)	1.75	121
256x256	c (1)	8.16	1024
	c (2)	7.50	961
	c (3)	5.85	729
	c (4)	4.46	576

512x512	d (1)	21.82	2809
	d (2)	19.99	2601
	d (3)	15.63	2025
	d (4)	11.56	1444

Table 1 presents the number of pixels at every step of the preprocessed image results. This table demonstrate the various dimensional images of the breast cancer affected patient with differences in pixel rates. The table also shows the variation from the original images as well as the resized images. Also, table 1 indicates how much memory space was utilized in storing the photos of varying sizes.

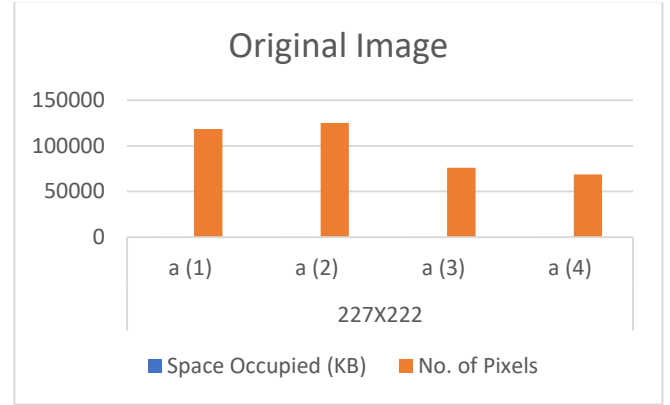


Figure 3. Pixel Rate of original image

Figure 3 gives a detailed view of the utilized memory space of the original images and pixel generated with the images. The simulations carried out to examine the pixel size as well as the memory utilized.

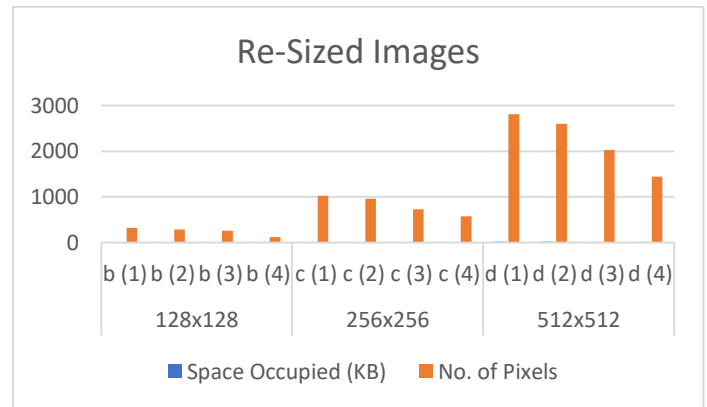


Figure 4. Pixel Rate of re-sized images

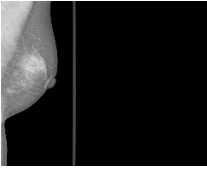
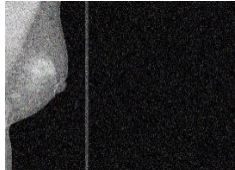
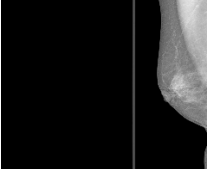

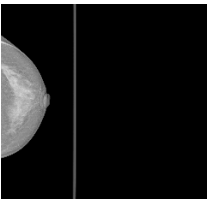
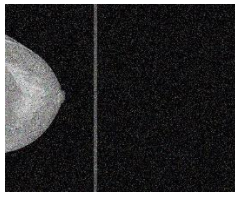
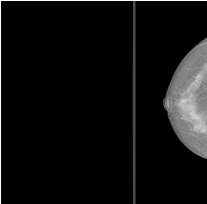

Figure 4 gives a detailed view of the utilized memory space of the various stages breast cancer affected patient and pixel generated with the images. The similar initial inspection and simulations are carried out to examine the pixel size as well as the memory utilized. The figure gives a detailed view of better utilization.

### Result for Salt and pepper noise Removal

Dark pixels will be in light regions and light pixels in dark regions of an image contaminated with salt and pepper noise.

This is because of dead pixels, transmission bit errors, and analogue to digital conversion problems. Dark frame elimination and interpolation at dark bright pixels can be applied to eliminate it.

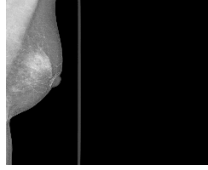

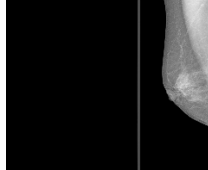

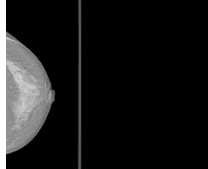

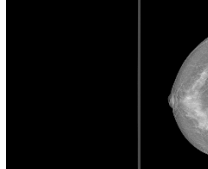
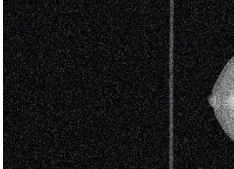
TABLE II. SALT AND PEPPER NOISE REMOVAL

P1 Gray Scale right view 	Salt and pepper P1 right view 
P1 Gray Scale left view 	Salt and pepper P1 left view 
P2 Gray Scale right view 	Salt and pepper P2 right view 
P2 Gray Scale left view 	Salt and pepper P2 left view 

**Result of Gaussian Low pass filter**

Every pixel in the image will be altered from its initial value by a (typically) little amount throughout the Gaussian noise removal process. As seen below, low pass filtering uses a compression technique to eliminate noise. This research explores the application of the Gaussian Low Pass Filter at the preprocessing step of image processing in breast cancer diagnosis. For suspicious region detection, discriminative feature extraction, and classification of the filtered images using the correct machine learning or deep learning algorithms, they are further processed. The final aim is to utilize automated image analysis to enhance diagnostic accuracy and help doctors in early breast cancer detection.

TABLE III. GAUSSIAN LOW PASS FILTER

P1 Gray Scale right view 	Gaussian Low Pass filtering P1 right view 
P1 Gray Scale left view 	Gaussian Low Pass filtering P1 left view 
P2 Gray Scale right view 	Gaussian Low Pass filtering P2 right view 
P2 Gray Scale left view 	Gaussian Low Pass filtering P2 left view 

**Result of Gaussian High pass filter**

Statistical noise with a normal distribution probability density function (pdf) also known as the Gaussian distribution is called Gaussian noise. Each pixel in the image will be changed from its original value by a (usually) small amount when there is Gaussian noise. As can be seen below, Gaussian High Pass employs inverse filtering to perform the deconvolution.

technique employed in medical imaging to generate better-quality black-and-white images. (Digital X-rays, CT scans, and MRIs)

TABLE IV. GAUSSIAN HIGH PASS FILTER

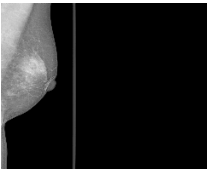
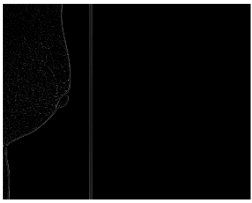
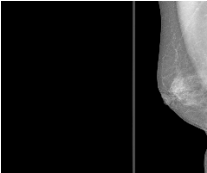
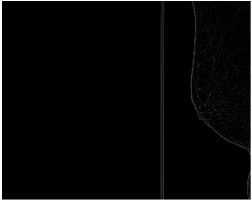
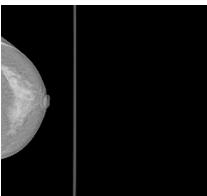
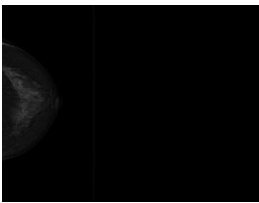
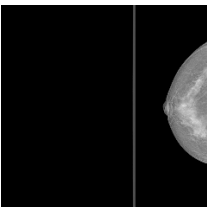
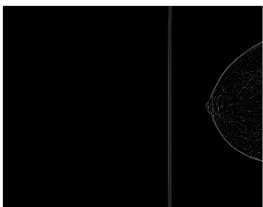
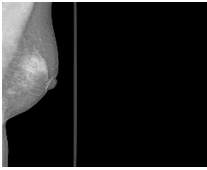
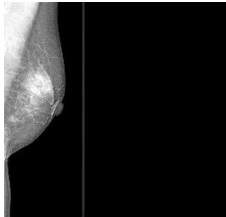
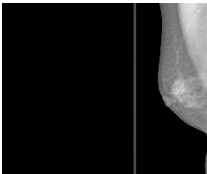
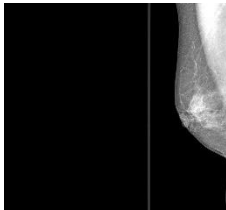
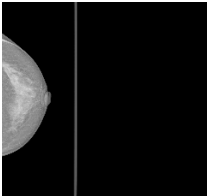
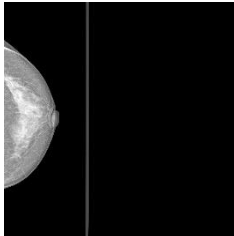
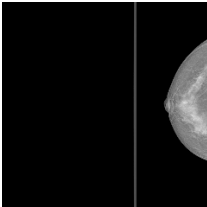
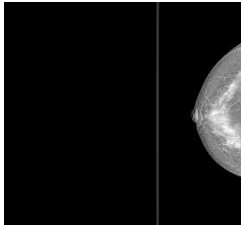
P1 Gray Scale right view 	Gaussian High Pass filtering P1 right view 
P1 Gray Scale left view 	Gaussian High Pass filtering P1 left view 
P2 Gray Scale right view 	Gaussian High Pass filtering P2 right view 
P2 Gray Scale left view 	Gaussian High Pass filtering P2 left view 

TABLE V. THE PERFORMANCE OF HISTOGRAM EQUALIZATION

P1 right view Before Contrast Enhancement 	P1 right view After Contrast Enhancement 
P1 left view Before Contrast Enhancement 	P1 left view After Contrast Enhancement 
P2 right view Before Contrast Enhancement 	P2 right view After Contrast Enhancement 
P2 left view Before Contrast Enhancement 	P2 left view After Contrast Enhancement 

**Result of Histogram Equalization**

The contrast of a greyscale image can be adjusted through histogram equalisation. Most of the pixel values of the original image occur within the middle of the intensity range, which means the image has low contrast. The pixel values in the resulting image are spread evenly throughout the range. Histogram equalisation is a straightforward image-processing

The Filtering Techniques Wiener Filter, Median Filter and Gaussian Low and High Pass Filter are deployed with various methods. The Result obtained can be clearly observed from Table VI. The observed results are very clear in explaining the

size variation of image and techniques deployed can alter the image clarity.

TABLE VI. FILTERING TECHNIQUES AND RESULT OBSERVED

Method	Filtering Technique	Results Observed
128 X 128	Wiener Filter	Small size and Dark
	Median Filter	Small size and Bright
	Gaussian Low and High Pass Filter	Small size and Clear
256 X 256	Wiener Filter	Medium size and Dark
	Median Filter	Medium size and Bright
	Gaussian Low and High Pass Filter	Medium size and Clear
512 X 512	Wiener Filter	Large size and Dark
	Median Filter	Large size and Bright
	Gaussian Low and High Pass Filter	Large size and Clear

The implementation of filtering process enhancement techniques, overlapping histogram equalisation is adapted and used with histogram equalization as in Table VI.

## CONCLUSION

The particular part of the research work focuses on the cleaning stage of the breast cancer Mammography images. The technique deployed in this part of the research work removes the irrelevancy in images as well as helps in improving the quality of the Mammography images. Various filtering techniques are implemented for enhancing the quality of the pre-processed mammography images. The sample breast cancer of two different patents is shown in the experimental results. The results are studied, compared against a normal pattern of noise, and evaluated as per quality. The aim of this research work is to focus on choosing appropriate filtering techniques and removing noise keeping in mind the phases of breast cancer images. Apart from reducing time, the preprocessing method considers the three varieties of filter types and searches for the best pixel outcome using the median filter. Furthermost, the preprocessed and enhanced images are taken for the next analyzing stage with proposed algorithm to identify the breast cancer affected parts from the Mammography images.

## References

[1] Sheikh, Hamid R., and Alan C. Bovik. "Image information and visual quality". *IEEE Transactions on image processing* vol.15(2), pp: 430-444, 2006

[2] S. Charan, M. J. Khan, and K. Khurshid, "Breast cancer detection in mammograms using convolutional neural network," in 2018 International Conference on Computing, Mathematics and Engineering Technologies (iCoMET). IEEE, 2018, pp. 1–5.

[3] H. Cai, Q. Huang, W. Rong, Y. Song, J. Li, J. Wang, J. Chen, and L. Li, "Breast microcalcification diagnosis using deep convolutional neural network from digital mammograms," *Computational and Mathematical Methods in Medicine*, vol. 2019, pp. 1–10, 03 2019.

[4] L. Tsochatzidis, L. Costaridou, and I. Pratikakis, "Deep learning for breast cancer diagnosis from mammograms—a comparative study," *Journal of Imaging*, vol. 5, no. 3, p. 37, 2019.

[5] Y.-D. Zhang, S. C. Satapathy, D. S. Guttery, J. M. Górriz, and S.-H. Wang, "Improved breast cancer classification through combining graph convolutional network and convolutional neural network." *Information Processing Management*, vol. 58, no. 2, p. 102439, 2021. [Online]. Available: <http://www.sciencedirect.com/science/article/pii/S0306457320309328>

[6] S. Tanini, A. D. Fisher, I. Meattini, S. Bianchi and J. Ristori, "Testosterone and breast cancer in transmen: Case reports, review of the literature, and clinical observation," *Clinical Breast Cancer*, vol.19,no.2,pp.e271–e275, 2018.

[7] R. L. Siegel, K. D. Miller and A. Jemal, "Cancer statistics," *CA Cancer Journal for Clinicians*, vol. 68, no. 1, pp. 7–30, 2018.

[8] S. A. Narod, "Tumour size predicts long-term survival among women with lymph node-positive breast cancer," *Current Oncology*, vol. 19, no. 5, pp. 249–253, 2012.

[9] A. B. Miller, C. Wall, C. J. Baines, P. Sun et al., "Twenty-five year follow-up for breast cancer incidence and mortality of the Canadian National Breast Screening Study: Randomised screening trial," *British Medical Journal*, vol. 348, pp. 366, 2014.

[10] R. M. Rangayyan, F. J. Ayres and J. E. L. Desautels, "A review of computer-aided diagnosis of breast cancer: Toward the detection of early signs," *Journal of the Franklin Institute*, vol. 344, no. 3/4, pp. 312–348, 2007.

[11] D. E. Goodman, L. C. Boggess and A. B. Watkins, "Artificial immune system classification of multiple-class problems," *Proceedings of the Artificial Neural Network in Engineering Systems*, vol. 12, pp. 179–186, 2004.

[12] J. R. Quinlan, "Improved use of continuous attributes in C4.5," *Journal of Artificial Intelligence Research*, vol. 4, pp. 77–90, 1996.

[13] D. Nauck and R. Kruse, "Obtaining interpretable fuzzy classification rules from medical data," *Artificial Intelligence in Medicine*, vol. 16, no. 2, pp. 149–169, 1999.

[14] G. I. Salama, M. B. Abdelhalim and M. A. Zeid, "Breast cancer diagnosis on three different datasets using multi classifiers," *International Journal of Computer and Information Technology*, vol. 1, pp. 36–43, 2012.

[15] H.J. Hamilton, N. Shan and N. Cercone, "RIAC: Arule induction algorithm based on approximate classification," *Technical Report*, <http://citeseerx.ist.psu.edu/viewdoc/download?doi=10.1.1.7.7768&rep=rep1&type=pdf>, 1996.

[16] K. Polat and S. Günes, "Breast cancer diagnosis using least square support vector machine," *Digital Signal Processing*, vol. 17, no. 4, pp. 694–701, 2007.

[17] A. Mert, N. Z. Kılıç, E. Bilgili and A. Akan, "Breast cancer detection with a reduced feature set," *Computational and Mathematical Methods in Medicine*, pp. 1–11, Article ID 265138, 2015.

[18] J. Dheeba, N. A. Singh and S. T. Selvi, "Computer-aided detection of breast cancer on mammograms: A swarm intelligence optimized wavelet neural network approach," *Journal of Biomedical Informatics*, vol. 49, no. 2, pp. 45–52, 2014.

[19] A. M. Abdel-Zaher and A. M. Eldeib, "Breast cancer classification using deep belief networks," *Expert Systems with Applications*, vol. 46, pp. 139–144, 2016.

[20] Marouene Chaieb, Malek Azzouz, Mokhles Ben Refifa, and Mouadh Fraj. 2025. Deep learning-driven prediction in healthcare systems: Applying advanced CNNs for enhanced breast cancer detection. *Comput. Biol. Med.* 189, C (May 2025).

[21] Byng, D. et al. AI-based prevention of interval cancers in a national mammography screening program. *Eur. J. Radiol.* 152, 110321 (2022).

[22] Ahmad, S., Zafar, I., Shafiq, S. et al. Deep learning-based computational approach for predicting ncRNAs-disease associations in metaplastic breast cancer diagnosis. *BMC Cancer* 25, 830 (2025)